Non Equilibrium Structured Polynuclear-metal-oxide Assemblies

Leroy Cronin

School of Chemistry, University of Glasgow, WestCHEM,
Glasgow, G12 8QQ, United Kingdom

E-Mail: Lee.Cronin@glasgow.ac.uk

Abstract

One pot reactions are deceptively simple systems often yielding complex mixtures of compounds, nanomolecular self-assembled architectures and intricate reaction networks of interconnected mutually dependent processes. As such, the elucidation of mechanism and various reaction pathways can be hard if not impossible to deduce. Herein, I show how by moving a 'one-pot' reaction from the time domain into a flow-system, the time domain translates into distance and flow rate thereby allowing monitoring and control of one-pot reactions in new ways; for example by changing the tube length/diameter. Three types of flow system are presented: (i) a system for the trapping of an intermediate host guest complex responsible for the formation of the giant wheel cluster which is the major component of molybdenum blue; (ii) a linear flow system array for the scale up of inorganic clusters; (iii) a networked reactor system which allowed the combination of multiple one-pot conditions in a single system allowing the discovery of a fundamental new class of inorganic cluster not accessible by any other means. I also briefly describe our recent work on the growth of inorganic tubules and our 3D printed 'reactionware' for the fabrication of bespoke flow-systems at a fraction of the cost of commercial systems and also show how the ability to configure the systems in new ways leads to new science.

Introduction

The discovery and synthesis of complex chemical nanostructures, both molecular and supra-molecular, is both time consuming and limited by lack of reproducibility, amount of material, and dependence on initial starting conditions. However, flow system approaches, utilized a lot in organic synthesis, have not been utilized for the synthesis of supramolecular and nanomolecular chemistry. Continuous flow processing in synthetic organic chemistry has many benefits and has been well researched and documented in recent years [1, 2]. Key advantages include higher heat transfer efficiencies, rapid and homogeneous mixing and this can lead to higher reaction rates with less side products, and consequently higher yields and selectivities [3, 4]. Continuous flow process techniques have also proved useful in a limited number of hard nanomaterials but examples are limited mainly to the production of metallic and semiconductor nanoparticles and quantum dots [5]. Other major areas of interest in inorganic chemistry, such as coordination compounds and clusters such as polyoxometalates (POMs) [6, 7] (especially those with interesting optical, redox, and magnetic properties etc) [8 – 12], typically utilize batch syntheses and purification *via* crystallization. This means that the main role of the synthetic chemist is to systematically screen the reaction conditions for the reproduction and scale up of novel architectures must therefore cover a large area of synthetic space as it not only has to achieve conditions suitable for the target formation, but target crystallization as well [13]. Large number reaction arrays are therefore an inherent aspect in this process, which can be an extremely laborious and time consuming task when working solely under batch conditions, especially when exploring delicate multi-parameter self-assembly reactions aiming to produce supramolecular architectures. Indeed, the size of the parameter space can be so vast that even after chance 'batch-discovery' the re-discovery and scale up of the process to produce more than a few crystals of the product can be almost impossible on a limited time-scale. As such, this presents a critical bottleneck to the reliable synthesis of inorganic macromolecules with scientifically and technologically important physical properties, where the lack of phase-pure material prevents a rigorous investigation of the physical properties or exploitation of the properties in real world devices and applications.

Templating Gigantic Molecular Assembly

In one of our first flow system devices we aimed to probe the assembly mechanism of gigantic molecular nanoparticles such as the wheel-shaped $\{Mo_{154-x}\}$ (x = 0 – 14) (the mixed-valence molybdenum blue (MB) type) cluster family [14] which have interesting physical and chemical properties, which arises from their molecular nature, nanoscale size, and electronic properties [15]. Our idea was that the inorganic MB-macrocycles can only be formed around a templating cluster, which is built of the same building blocks as the macrocycle itself and therefore acts as a building blocks feedstock, during the process of macrocycle assembly but this was hard to prove as the MB type clusters are synthesised by the reduction of an acidic molybdate solution (pH 1 – 3) under static one-pot conditions

[16 – 20]. Under these conditions, the self-assembly of reactive $[Mo_xO_y]$-type building blocks (in the final structures mostly given as $\{Mo_1\}$, $\{Mo_2\}$, $\{(Mo)Mo_5\}$ and $\{Mo_8\}$, see Fig. 1) gives rise to $\{Mo_{154-x}\}$ ($x = 0 – 14$), which can be rationalized formally as assemblies of the above mentioned building blocks. Yet the reaction conditions effectively concealed the template required for the self-assembly process. We were able to deduce this by using a controllable dynamic synthetic procedure in a flow system such that it is possible to adjust the three input variables (pH, concentration of molybdate and reducing agent) which control the synthesis of the molecular nanosized-wheels in real time compared to the static synthetic approach, see Fig. 1.
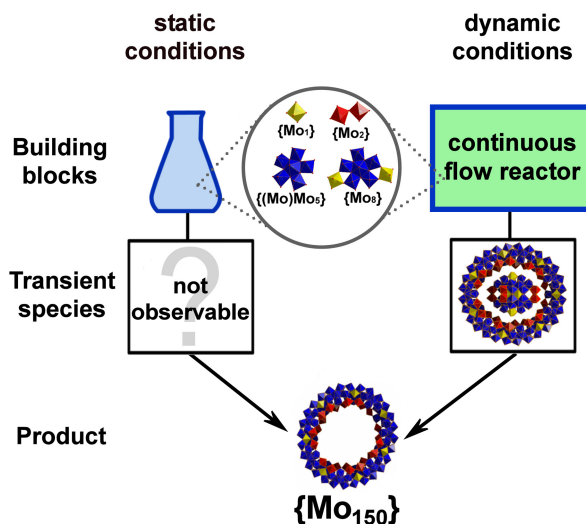
Figure 1. Polyhedral representation of the basic building units (present in the final structure) which govern the (soluble) molybdenum-oxide based, i.e. MB chemistry with giant clusters as well as schematic representation of the static and dynamic synthetic approach to assemble the 2.6 nm diameter molecular nano wheel. The transient species, the molecular wheel with the template 'X' is observed in a flow system crystallizer.

By utilising a flow-system, as opposed to the classical one-pot reaction, we are able to maintain the concentration of the transient by controlling the degree of reduction of the polyoxomolybdate reaction solution (see Fig. 2). As such the assembly of the MB architecture under controlled reduction conditions leads to the trapping of a $\{Mo_{150}\}$ wheel with a $\{Mo_{36}\}$ cluster template that is bound to the central cavity of the ring species *via* sodium cations. This host guest complex shows features indicative of an intermediate electronic and structural state, and we conclude that the $\{Mo_{36}\}$ cluster acts as the key template in the formation of the MB ring. The host guest complex is isolated as the crystalline compound $Na_{22}[Mo^{VI}_{36}O_{112}(H_2O)_{16}] \subset [Mo^{VI}_{130}Mo^{V}_{20}O_{442}(OH)_{10}(H_2O)_{60}] \cdot 180\,H_2O$ in the flow-system by the reduction of an aqueous acidic solution of $Na_2MoO_4 \cdot 2\,H_2O$ with $Na_2S_2O_4$ under

continuous addition of HNO_3 in a gram yield. The use of nitric acid in the flow system is important as it has the dual role of a proton source, and as an oxidant causing incomplete reduction of the wheel. The "normal", i.e. complete/symmetrical wheel $\{Mo_{154}\}$ has 14 two-electron reduced compartments (i.e. with a total of 28 4d electrons) but here only 10 of the 14 compartments are two-electron reduced with the wheel being a total of 20-electron reduced.
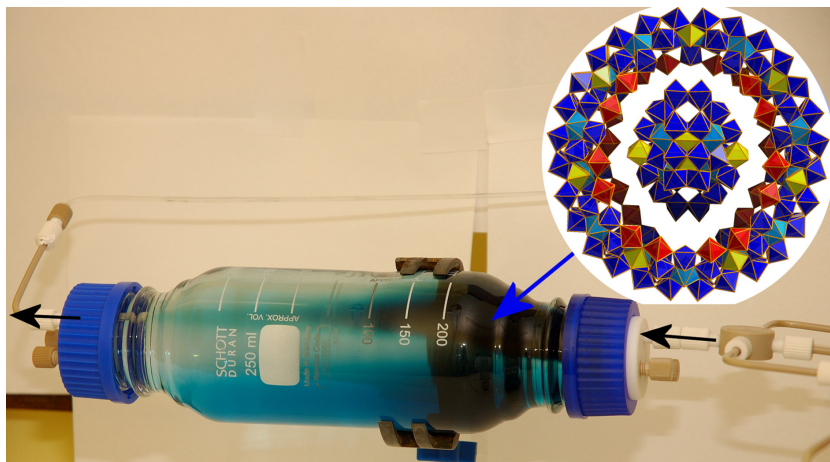
Figure 2. Photograph of the flow system with the reduced molybdenum blue and a polyhedral representation of the templated $\{Mo_{36}\} \subset \{Mo_{150}\}$ ring which crystallizes from the flow reactor.

## 'ONE-POT' REACTIONS OF POLYOXOMETALATE SYNTHESIS IN LINEAR FLOW SYSTEM ARRAYS

In this approach we took the multiple input 'ingredients' normally added to the 'one-pot' reaction systems and made up each ingredient as a separate flow input into a reaction chamber where the number of inputs into the reaction chamber is normally equal to the number of distinct reagents used in the stand alone 'one-pot' reaction. By using a continuous flow processing with batch crystallization over a set array, we were able to devise a new efficient method for creating large number reaction arrays for rapidly scanning large areas of reaction parameter space to increase the probability of discovering new materials. Also, this flow based approach for the generation of multiple batch reactions can be used for the continuous production of identical batch reactions required for scale-up of the isolated materials. We were able to validate this approach by setting up a multiple pump reactor system for the synthesis of a range polyoxomolybdates of various sizes and structural complexity, $\{Mo_x\}$ compounds shown in figure 3 [13–16]. The setup utilized twelve programmable syringe pumps, although this is extendable to fifteen in our system, and a PC interface was used for controlling the pumps (Fig. 1.).

The reagent set chosen for POM synthesis consisted of distilled deionized water for dilution, 2.5 M $Na_2MoO_4 \cdot 2\,H_2O$ as the molybdenum source, three acid sources (5.0 M HCl, 1.0 M H_2SO_4, and 50% AcOH), 4.0 M $AcO(NH_4)$, and two sources of reducing agent, 0.25 M $Na_2S_2O_4$ and saturated (0.23 M) $N_2H_2 \cdot H_2SO_4$. For the simplest POM target, compound $\{Mo_{36}\}$, only three of the twelve pumps were required to incrementally vary the relative flow rates of the water, molybdate and HCl stock solutions; for the $\{Mo_{154}\}$, $\{Mo_{132}\}$, $\{Mo_{102}\}$, and $\{Mo_{368}\}$ compounds up to five pumps were required to supply the additional reducing agent and buffer stocks [21]. In the example of the synthesis of the $\{Mo_{36}\}$ compound, this involves acidifying an aqueous solution of sodium molybdate, which subsequently precipitated crystals of the target compound, and we prepared a pump setup that could repeat this screening process. With $\{Mo_{36}\}$ for our ''screening array'', the pumps were programmed to run at a range of flow rates, incrementally increasing both the relative ratio of acid to molybdate and the overall reagent concentrations (two key parameters of POM formation and crystallization) throughout the experimental run. In this case variation of just these two parameters resulted in the creation of fifty distinct reaction batches with the potential to crystallise the $\{Mo_{36}\}$ target and crucially the successful systems could be repeated many times reliably to allow the isolation of many grams of material if required.

'ONE-POT' REACTIONS OF POLYOXOMETALATE SYNTHESIS IN NETWORKED REACTION SYSTEMS

One important problem is that 'one-pot' reactions mask a vast and complex range of intricate self-assembly processes that must invariably occur in solution, and it is therefore difficult to predict or control the assembly process. This issue is not limited to polyoxometalates, but extends to a vast number of other chemical systems e.g. supramolecular, nanoparticles, DCLs and coordination chemistry. To go beyond our previous work we theorised that it could be possible to systematically explore the systems by doing combinatorial reactions one-by-one, but this only probes the combinatorial space in a very limited sense. However, the rapid screening and integration of a large number of 'one-pot' reactions would be transformative since this would allow both the compositional and time dependent space to be integrated, and 'networked', and we recently proposed this and published the first example of such a set up experimentally, see figure 4 [22].
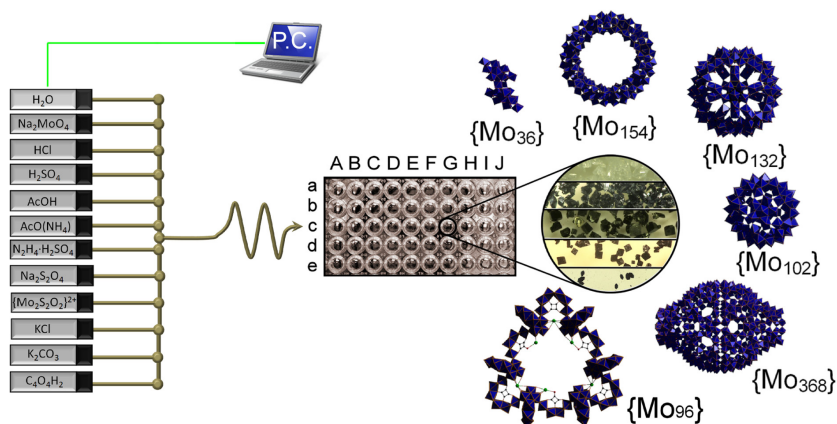
Figure 3. Reaction input parameters were altered to generate reaction arrays that were screened for the crystallization of polyoxomolybdate targets. A schematic of the pump setup and reagent inputs (left) leads to a representative image of the 5×10 reaction array outputs (centre). During the screening process for each target, crystal batches were obtained in a handful of reactions where the flow conditions produced the reaction conditions required for successful crystallization. Images of crystal batches and polyhedral structural representations for the target polyoxomolybdates are shown (right). The truncated molecular formulae in parentheses represent the following complete formulae: $\{Mo_{36}\} = Na_8[Mo_{36}O_{112}(H_2O)_{16}] \cdot 58 H_2O$; $\{Mo_{154}\} = Na_{15}[Mo^{VI}_{126}Mo^{V}_{28}O_{462}H_{14}(H_2O)_{70}]_{0.5}[Mo^{VI}_{124}Mo^{V}_{28}O_{457}H_{14}(H_2O)_{68}]_{0.5} \cdot ca. 400 H_2O$; $\{Mo_{132}\} = (NH_4)_{42}[Mo^{VI}_{72}Mo^{V}_{60}O_{372}(CH_3COO)_{30} (H_2O)_{72}] \cdot ca. 300 H_2O \cdot ca. 10CH_3COONH_4$; $\{Mo_{102}\} = Na_{12}[Mo^{VI}_{72}Mo^{V}_{30}O_{282}(SO_4)_{12}(H_2O)_{78}] \cdot ca. 280 H_2O$; $\{Mo_{368}\} = Na_{48}[H_xMo_{368}O_{1032}(H_2O)_{240}(SO_4)_{48}] \cdot ca. 1000 H_2O$; and $\{Mo_{96}\} = (N(CH_3)_4)_6K_{30}\{ [(Mo_2O_2S_2)_3(OH)_4(C_4O_4)]_9[(Mo_2O_2S_2)_2(OH)_2(C_4O_4)]_3 (Mo_5O_{18})_6\} \cdot 132 H_2O$.
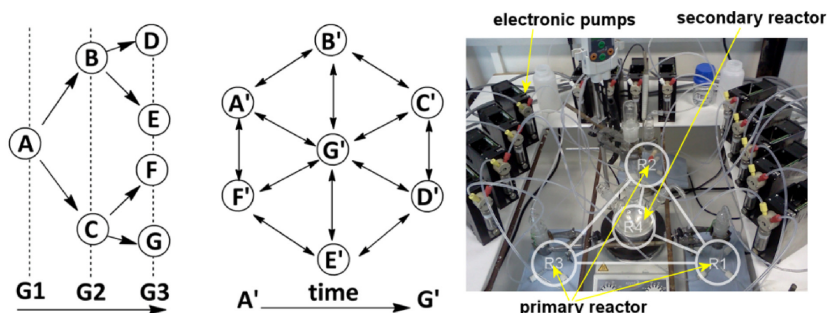

Figure 4. Left: comparison between conventional parameter space, a, (i. e. generations G1, G2 and G3) and networked multiple parameter, b, screenings, in X or X' 'one-pot' reactions (where X = A to G). Right: photograph of the physical networked 'one-pot' reactor array, c.

Thus the development of a networked 'one-pot' reaction array (Fig. 4c) should be of fundamental importance since linking multiple complex assembly processes, such as those found in one-pot systems, provides potential not only for the reproducible assembly of complex nanostructures, but also allows the systematic combination of one-pot reactions of similar systems as a function of time or composition permitting the exploration of virtual libraries of building blocks. Potentially this could lead to the control of assembly at the molecular level using 'macro-control' in a series of 'one-pot' reactions connected in a flow system [22].

By designing and setting up a Networked Reactor System (NRS) for the discovery of polyoxometalate clusters, we applied this approach to the synthesis of an unknown family of metal-containing isopolyoxotungstates (iso-POTs) in presence of templating transition metals such as Co^{2+}, see figure 5, by screening networks of 'one-pot' reactions. This shows that the NRS approach can lead to the discovery of new clusters in a reproducible way allowing one-pot reactions to be probed or expanded over a number of reaction vessels, rather than relying on one single vessel. As such, the use of the NRS leads to the discovery of a chain-linked iso-POT $\{(DMAH)_6[H_4CoW_{11}O_{39}]\bullet6\,H_2O\}_n \equiv \{W_{11}Co\}_n$, a Co-trapped iso-POT $Na_4(DMAH)_{10}\,[H_4CoW_{22}O_{76}(H_2O)_2]\bullet20\,H_2O \equiv \{W_{22}Co\}$ and, $Na_{16}(DMAH)_{72}$ $[H_{16}Co_8W_{200}O_{660}(H_2O)_{40}]\bullet ca600\,H_2O \equiv \{W_{200}Co_8\}$ which is over 4 nm in diameter and it represents the largest discrete polyoxotungstate cluster so far characterized [22]. This cluster is formed uniquely in the NRS since several different one-pot reaction processes can be set up independently and mixed together leading to the interconnection of building blocks synthesized in the network of reactors which are then linked to yield the final cluster compounds.
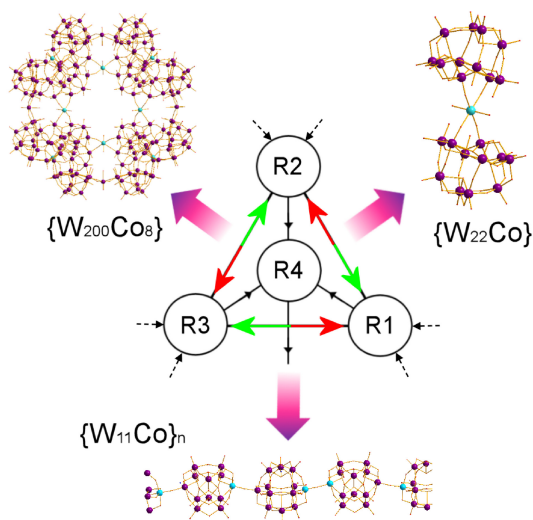
Figure 5. Scheme of Networked Reactor System (red and green arrows show the clockwise and anticlockwise circulation of the 'one-pot' reactions) and the new structures are highlighted around the triangle-shaped networked reactor system: Crystal structures of compounds $\{W_{11}Co\}_n$, $\{W_{22}Co\}$ and $\{W_{200}Co_8\}$ are shown in ball and stick mode. Colour scheme: W purple, Co cyan, O red.

The discovery of the $\{W_{200}\}$ is accomplished uniquely in the NRS which is interesting since this opens the way for nanoscale control using macro-scale parameters. This is because the NRS is designed to combine two aspects: the synthesis of new compounds by linking separate 'one-pot' reactions each containing unique building blocks, (BBs) followed by the mixing of these individual 'one-pot' reactions i. e. moving the regents from reactor to reactor. Thus the NRS allows control in both reaction in both *time* and *space* (by comparison we consider that normal 'one-pot' reactions only search in time). As such three primary reactors, each with two external reagent inputs, are connected together in a triangular arrangement with a central secondary reactor (connecting to all three primary reactors), defining the simplest implementation of the NRS. As the NRS has a high connectivity, this allows a wide range of multiple mixing pathways in which the reagents can move from one flask to another (i. e. anti-clockwise R1→ R2→ R3→ R4 or clockwise R1→ R3→ R2→ R4). This allows the recycling and re-feeding processes according to $(R1 → R2 → R3)_n$ (n = number of cycles) depending of standard flow parameters in the NRS. In contrast to a linear setup, the NRS allows many different reagent inputs to be accommodated in separate reactors. Moreover, the system can allow both the screening and automation of the syntheses over a range of different clusters by selecting the reaction and flow parameters (flow rates, pH, initial volumes, etc.) in a highly automated, controlled and reproducible manner.
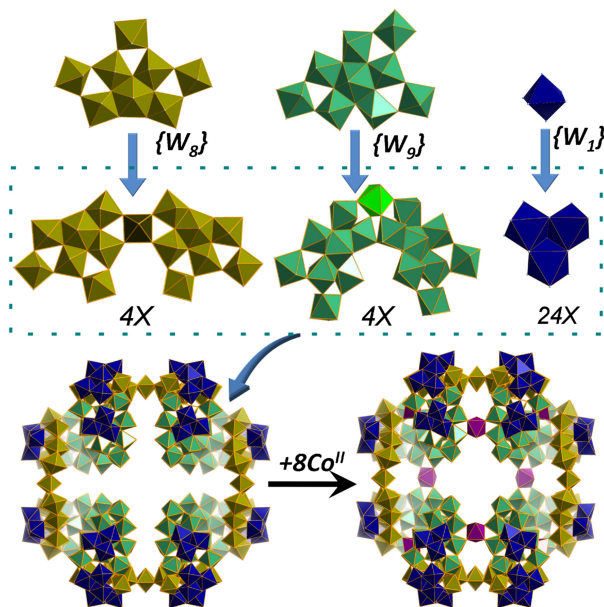
Figure 6. Representation of the crystal structure of the $\{W_{200}\}$. The three principal building blocks are represented at the top, where $\{W_8\}$ and $\{W_9\}$ are derived from $\{W(W)_5\}$ pentagonal unit. Following to principal BBs, the secondary BBs are represented in the middle section, as result of condensation of primary building blocks. Finally, the compound is completed by the complexation of 8 cobalt ions.

The gigantic isopolyanion compound $\{W_{200}Co_8\}$, is a saddle-shaped structure and contains unusual pentagonal units and crystallizes as a hydrated sodium and dimethylammonium salt of $\{H_{16}Co_8W_{200}O_{660}(H_2O)_{40}\}^{88-}$ and single crystal X-ray diffraction shows the crystals belonging tetragonal system with space group of $P4_2/nmc$. The cluster itself has an approximate D_{2d} symmetry and the building blocks are highlighted in figure 6.

Thus our idea of the networked reactor system (NRS) has been realised where multiple one-pot connected reactions are screened, the reaction variables explored, and automation of the syntheses of three compounds was achieved. The potential of the NRS methodology is transformative due to the ability to explore one-pot reactions as configurable modules, and to explore different mixing and reaction conditions in a programmed and sequential way (stepwise process) as well as allowing the combination of building block libraries that could not coexist in classical one-pot reactions. This is because the NRS allowed the combination of pH adjustment/UV monitoring in real time, thus confirming different local experimental conditions in each reactor within the system. This feature makes the NRS potentially very useful to explore other combinations of initial reagents, to study reaction mechanisms and self-assembly reactions in other areas of chemistry (i.e. coordination chemistry or design of metal-organic frameworks). As such, we demonstrate 'macroscale' control of the assembly of polyoxometalates for the first time, and this builds on our observations of 'microscale' control of assembly and opens perspectives to utilise the approach here in exploring 'assembly-isomers' of polyoxometalates in the NRS, as well as providing radically new structures (very high charge).

GROWTH OF INORGANIC MICROTUBES FROM POLYOXOMETALATES

Initially reported by us in 2009, the growth of micron-scale hollow tubes from polyoxometalate (POM) materials undergoing cation exchange with bulky cations in aqueous solution has now been shown as a general phenomenon for POMs within a critical solubility range. While it is not a classical chemical garden process, there are many similarities in the growth mechanism [23 – 27]. Although POMs have much in common with bulk transition metal oxides, their molecular nature means they have a vast structural diversity with many applications as redox, catalytically active and responsive nanoscale materials. Tube growth has been demonstrated with a wide range of different cations including several dihydro-imidazo-phenanthridinium (DIP) compounds, 3,7-bis(dimethylamino)-phenothiazin-5-ium chloride (methylene blue), polymeric poly(N-[3-(dimethylamino)propyl]methacrylamide) and even the complex $Ru^{II}(bipy)_3(BF_4)_2$ (bipy = 2,2'-bipyridyl). When dissolved anionic POM fragments, with their associated small cations, come into contact with bulky cations in solution, ion exchange occurs and the resulting aggregates grow sufficiently large to become insoluble. Due to the charge to size ratios of the molecules involved, it is often not favourable to make a fully charge balanced species, and so the material tends to be 'sticky', which results

in continued aggregation to form precipitation membranes. When the dissolved POM material is introduced to the cation solution via a small aperture this tendency results in the formation of a continuous hollow (tube) structure, see figure 7.
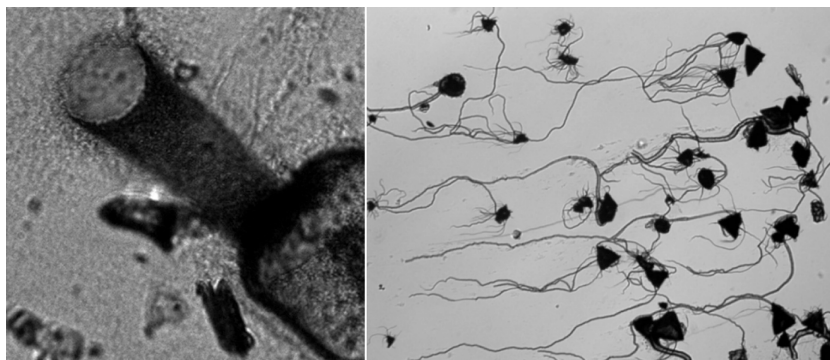

Figure 7. Growth of a microtube (approx. 50 μm diameter) growing on a glass surface. $(C_4H_{10}NO)_{40}[W_{72}Mn_{12}O_{268}Si_7]\cdot48\,H_2O$ POM in N-methyl dihydroimidazolphenanthridinium bromide solution. Right: Growth of several microtubes (approx. 25 – 75 μm diameter) under bulk flow conditions showing the alignment of the growth direction to the flow.

The tube continues to grow from the open end until the source of POM material is exhausted, a shorter exit route is provided (e. g. from a rupture in the tube closer to the source), or the cation concentration becomes too low for aggregation. In general, the POM solutions are denser than the cation solutions, and so the microtubes grow along the bottom surface of their sample container. However, when the solution densities are closely matched or the sample volume is very small, the tubes will 'climb' along the sample container walls or any other introduced obstacles, or can be seen to grow vertically into the solution.

In order to make useful patterns or devices from POM microtubes, their characteristics must be controllable. As the POM material flows from the end of the growing tube, the rate of aggregation is strongly influenced by the local availability (concentration) of cations and the rate of outflow. When the rate or concentration is increased, the material begins to aggregate more rapidly and the resulting tube narrows. The opposite is true if the rate or concentration is reduced. In the case of tubes growing from a crystal, the outflow is essentially fixed, as the surface area of the membrane (and thus the rate at which water can cross it) does not change. Since the POM material is of low solubility, the POM solution within the membrane and tube will be at saturation. This is not the case when the tube is grown by microinjection, since the pressure can be varied and this allows a direct control over the diameter.

As the POM material is ejected from the growing tube, it is influenced by any liquid flow in the sample such that tubes will always grow along the direction of flow. In a bulk sample, the use of electrodes to set up convection currents allows the direction of the growing tubes to be controlled. However, this does not allow the production of any useful network or tube-

based device as the control is exerted on all the tubes simultaneously (see figure 8 RHS). By using a dye molecule in the cation solution, a focused laser spot can be used to create a localized flow; at the laser spot, the solution is heated and this creates an upward flow. To relieve the low pressure that this generates, there is a localized flow towards the focused spot. Any growing microtubes in the vicinity are then pulled towards the spot and by moving the spot the growth direction can be controlled. This means that an individual tube can be steered reliably and independently. By coupling the laser optics to a spatial light modulator (SLM) in a setup more commonly used as 'optical tweezers', the laser light can be split into multiple foci which can be used to control different growing tubes independently within the same sample. Growing a specific structure requires accurate positioning of the laser spots by a user who can react to the progress of the system, and this depends critically on the computer interface used to control the SLM. To achieve this, the microscope image is displayed on a multi-touch tablet (Apple iPad), along with markers representing the laser spots. These markers can be dragged around, moving the laser spots to follow the user's fingers, so that multi-touch gestures allow the growing microtubes to be controlled (examples of structures in figure 8 left). The laser heating also allows tube walls to be deliberately ruptured, producing branch points, or pre-loaded capillaries to be un-blocked in-situ so that extra tubes can be initiated on demand during 'device' construction. It is also possible to automate the movement of the laser spot with image analysis and feedback such that the computer can control the laser spot to steer a microtube into a predefined pattern as it grows (see Fig. 8 right).
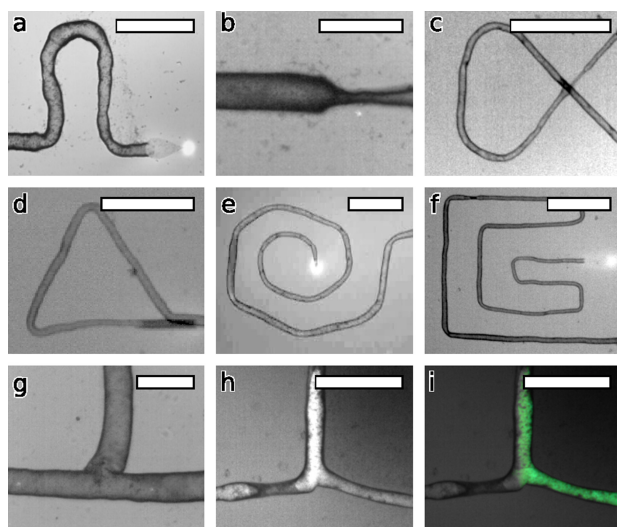

Figure 8. The holographic system can produce devices using a number of basic elements of the inorganic micro networks: **(a)** a sharp bend (scale bar 100 μm), **(b)** a change in diameter (scale bar 100 μm), **(c)** tubes crossing over one another (scale bar 500 μm), **(d)** a triangle motif (scale bar 250 μm), **(e)** a spiral pattern (scale bar 500 μm), **(f)** a nested pattern (scale bar 500 μm), **(g)** a 'T' junction produced by puncturing a growing tube (scale bar 100 μm), **(h)** a 'Y' junction produced by merging two tubes (scale bar 250 μm) and **(i)** a similar 'Y' junction where green fluorescent dye (Fluorescein) is introduced into one of the tubes (scale bars = 500 μm).

3D Printed 'Reactionware' as Configurable Flow System Devices

Traditionally, the fabrication of flow devices and their interfacing with in-line analysis is complicated and expensive as micro-scale fluidic devices have been required. We have been working on a convergent approach developing 3D-printed milli-scale flow devices, or tailored "reactionware" for chemical reactions and in-line analysis [28, 29]. The use of three-dimensional (3D) printing bypasses sophisticated manufacturing centres, and promises to revolutionise every part of the way that materials are turned into functional devices, from design through to operation, with 3D printing producing bespoke, low-cost appliances which previously required dedicated facilities. 3D printing is a cheap chemical discovery tool which combines the disciplines of synthetic chemistry and chemical engineering in a re-configurable and highly accessible format. The use of freely available CAD software and the rapid fabrication that comes with 3D printing, allows for the design and production of specific devices tailored to the intended chemical reaction. The high surface area-to-volume-ratio, precise control of volume and manipulation of reaction environment results in strict control of the final device, and the subsequent reactions carried out.

We have previously demonstrated the versatility and configurability of reusable and bespoke reactionware, where 3D printing was used to initiate chemical reactions by printing reagents directly into a 3D 'reactionware' matrix [29, 30]. We have also presented how 3D printing can be used to make intricate micro- and milli- scale reactionware for organic, inorganic and materials syntheses, offering significant freedom to design bespoke reactors in terms of residence time, mixing points, inlets and outlets, etc., see figure 9. For example in the reactor shown in figure 9, it is possible to synthesise Mo-blue as in the much larger and more difficult to control flow system shown in figure 2.
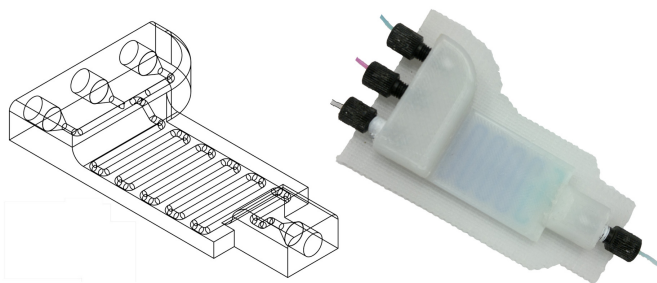
Figure 9. On the left is a schematic presentation of the .stl file, whilst on the right is the device with screw fittings and connected with 1/16th inch tubing. Methylene Blue and Rhodamine B are being pumped through the device, which allows for the inner tube-path to be rendered visible. A section consisting of only Methylene Blue can be seen at the front, followed by a stronger purple band, which is obtained from the successful mixing of Rhodamine B and Methylene Blue.

CONCLUSIONS

Molecular metal oxides based upon polyoxometalates are incredibly interesting compounds but they are extremely complex and the mechanism of assembly leading to real architectural control is far from reach under normal reaction conditions. To combat this problem we have developed new reaction approaches which allow the exploration of the self-assembly of complex molecular, supramolecular and nanomolecular species in fundamentally different ways to that traditionally envisaged by synthetic chemists. In particular the use of linear, branched, and networked flow systems to probe the fundamentals of molecular assembly is a new approach which promises to allow us to program the assembly of complex architectures by combining concepts from supramolecular chemistry, with reaction kinetics and non-equilibrium processing. Further, by developing optical guidance systems it is possible to grow physical structures of the metal oxides using computer control on the micron scale and finally the use of 3D printed 'reactionware' gives the ability to design new reactor systems with in-line analysis and new control approaches is now within reach.

ACKNOWLEDGEMENTS

REFERENCES

[1]   *Chemical Reactions and Processes under Flow Conditions*; Luis, S.V., Garcia-Verdugo, E., Eds.; Royal Society Chemistry: Cambridge, (2010).

[2]   Seeberger, P.H. (2009) Organic synthesis: scavengers in full flow. *Nat. Chem.* **1**:258 – 260.
        http://dx.doi.org/10.1038/nchem.267.

[3]   Wegner, J., Ceylan, S. & Kirschning, A. (2011) Ten key issues in modern flow chemistry. *Chem. Commun.* **47**:4583 – 4592.
        http://dx.doi.org/10.1039/c0cc05060a.

[4]   Hartman, R.L., McMullen, J.P. & Jensen, K.F. (2011) Deciding whether to go with the flow: evaluating the merits of flow reactors for synthesis. *Angew. Chem. Int. Ed.* **50**:7502 – 7519.
        http://dx.doi.org/10.1002/anie.201004637.

[5]   Abou-Hassan, A., Sandre, O. & Cabuil, V. (2010) Microfluidics in inorganic chemistry. *Angew. Chem. Int. Ed.* **49**:6268 – 6286.
        http://dx.doi.org/10.1002/anie.200904285.

[6] Long, D.-L., Burkholder, E. & Cronin, L. (2007) Polyoxometalate clusters, nano-structures and materials: from self assembly to designer materials and devices. *Chem. Soc. Rev.* **36**:105 – 121.
http://dx.doi.org/10.1039/b502666k.

[7] Long, D.-L., Tsunashima, R. & Cronin, L. (2010) Polyoxometalates: building blocks for functional nanoscale systems. *Angew. Chem. Int. Ed.* **49**:1736 – 1758.
http://dx.doi.org/10.1002/anie.200902483.

[8] Evangelisti, M. & Brechin, E.K. (2010) Recipes for enhanced molecular cooling. *Dalton Trans.* **39**:4672 – 4676.
http://dx.doi.org/10.1039/b926030g.

[9] Inglis, R., Milios, C.J., Jones, L.F., Piligkos, S. & Brechin, E.K. (2012) Twisted molecular magnets. *Chem. Commun.* **48**:181 – 190.
http://dx.doi.org/10.1039/c1cc13558a.

[10] Moushi, E.E. *et al.* (2010) Inducing single-molecule magnetism in a family of loop-of-loops aggregates: heterometallic $Mn_{40}Na_4$ clusters and the homometallic Mn_{44} analogue. *J. Am. Chem. Soc.* **132**:16146 – 16155.
http://dx.doi.org/10.1021/ja106666h.

[11] Murrie, M. (2010) Cobalt(II) single-molecule magnets. *Chem. Soc. Rev.* **39**:1986 – 1995.
http://dx.doi.org/10.1039/b913279c.

[12] Wang, X.-Y., Avendano, C. & Dunbar, K.R. (2010) Molecular magnetic materials based on 4 d and 5 d transition metals. *Chem. Soc. Rev.* **40**:3213 – 3238.
http://dx.doi.org/10.1039/c0cs00188k.

[13] Richmond, C.J., Miras, H.N., de la Oliva, A.R., Zang, H., Sans, V., Paramonov, L., Makatsoris, C., Inglis, R., Brechin, E.K., Long, D.-L., & Cronin, L. (2012) A flow-system array for the discovery and scale up of inorganic clusters. *Nature Chem.* **4**:1037 – 1043.
http://dx.doi.org/10.1038/nchem.1489.

[14] Müller, A. *et al.* (1999) Rapid and simple isolation of the crystalline molybdenum-blue compounds with discrete and linked nanosized ring-shaped anions: $Na_{15}[Mo^{VI}_{126}Mo^{V}_{28}O_{462}H_{14}(H_2O)_{70}]_{0.5}$ $[Mo^{VI}_{124}Mo^{V}_{28}O_{457}H_{14}(H_2O)_{68}]_{0.5}$ · ca. $400\,H_2O$ and $Na_{22}[Mo^{VI}_{118}Mo^{V}_{28}O_{442}H_{14}(H_2O)_{58}]$ · ca. $250\,H_2O$. *Z. Anorg. Allg. Chem.* **625**:1187 – 1192.
http://dx.doi.org/10.1002/(SICI)1521-3749(199907)625:7<1187::AID-ZAAC1187>3.0.CO;2-#.

[15] Miras, H. N. *et al.* (2012) Unveiling the transient template in the self assembly of a molecular oxide nano-wheel. *Science* **327**:72 – 74.
http://dx.doi.org/10.1126/science.1181735.

[16]   Müller, A., Krickemeyer, E., Bögge, H., Schmidtmann, M. & Peters, F. (1998) Organizational forms of matter: an inorganic super fullerene and keplerate based on molybdenum oxide. *Angew. Chem. Int. Ed.* **37**:3359 – 3363. http://dx.doi.org/10.1002/(SICI)1521-3773(19981231)37:24<3359::AID-ANIE3359>3.0.CO;2-J.

[17]   Krebs, B., Stiller, S., Tytko, K.H. & Mehmke, J. (1991) Structure and bonding in the high-molecular-weight isopolymolybdate ion, $(Mo_{36}O_{112}(H_2O)_{16})^{8-}$ – the crystal structure of $Na_8(MO_{36}O_{112}(H_2O)_{16}) \cdot 58 H_2O$. *Eur. J. Solid State Inorg. Chem.* **28**:883 – 903.

[18]   Müller, A., Beckmann, E., Bögge, H., Schmidtmann, M. & Dress, A. (2002) Inorganic chemistry goes protein size: a Mo_{368} nano-hedgehog initiating nanochemistry by symmetry breaking. *Angew. Chem. Int. Ed.* **41**:1162 – 1167. http://dx.doi.org/10.1002/1521-3773(20020402)41:7<1162::AID-ANIE1162>3.0.CO;2-8.

[19]   Müller, A. *et al.* (1995) $[Mo_{154}(NO)_{14}O_{420}(OH)_{28}(H_2O)_{70}]^{(25 \pm 5)-}$: A water-soluble big wheel with more than 700 atoms and a relative molecular mass of about 24000. *Angew. Chem. Int. Ed.* **34**:2122 – 2124. http://dx.doi.org/10.1002/anie.199521221.

[20]   Miras, H.N., Richmond, C.J., Long, D.-L. & Cronin, L. (2012) Solution-phase monitoring of the structural evolution of a molybdenum blue nanoring. *J. Am. Chem. Soc.* **134**:3816 – 3824. http://dx.doi.org/10.1021/ja210206z.

[21]   Miras, H.N., Yan, J., Long, D.-L. & Cronin, L. (2012) Engineering polyoxometalates with emergent properties. *Chem. Soc. Rev.* **41**:7403 – 7430. http://dx.doi.org/10.1039/c2cs35190k.

[22]   de la Oliva, A.R., Sans, V., Miras, H.N., Yan, J., Zang, H., Richmond, C.J., Long, D.-L. & Cronin, L. (2012) Assembly of a Gigantic Polyoxometalate Cluster $\{W_{200}Co_8O_{660}\}$ in a Networked Reactor System. *Angew. Chem. Int. Ed.* **51**:12759 – 12762. http://dx.doi.org/10.1002/anie.201206572.

[23]   Ritchie, C., Cooper, G.J.T., Song, Y.-F., Streb, C., Yin, H., Parenty, A.D.C., MacLaren, D.A., & Cronin, L. (2009) Spontaneous Assembly and Real-Time Growth of Micron-Scale Tubular Structures from Polyoxometalate-Based Inorganic Solids. *Nature Chem.* **1**:47 – 52. http://dx.doi.org/10.1038/nchem.113.

[24]   Cooper, G.J.T. & Cronin, L. (2009) Real-Time Direction Control of Self Fabricating Polyoxometalate-Based Microtubes. *J. Am. Chem. Soc* **131**:8368 – 8369. http://dx.doi.org/10.1021/ja902684b.

[25] Boulay, A.G., Cooper, G.J.T. & Cronin, L. (2012) Morphogenesis of polyoxometalate cluster-based materials to microtubular network architectures. *Chem Commun.* **48**:5088 – 5090.
http://dx.doi.org/10.1039/c2cc31194a.

[26] Cooper, G.J.T., Boulay, A.G., Kitson, P.J., Ritchie, C., Richmond, C.J., Thiel, J., Gabb, D., Eadie, R., Long, D.-L. & Cronin, L. (2011) Osmotically Driven Crystal Morphogenesis: A General Approach to the Fabrication of Micrometer-Scale Tubular Architectures Based on Polyoxometalates. *J. Am. Chem. Soc.* **133**:5947 – 5954.
http://dx.doi.org/10.1021/ja111011j.

[27] Cooper, G.J.T., Bowman, R.W., Magennis, E.P., Fernandez-Trillo, F., Alexander, C., Padgett, M.J. & Cronin, L. (2012) Directed Assembly of Inorganic Polyoxometalate-based Micrometer-Scale Tubular Architectures by Using Optical Control. *Angew. Chem. Int. Ed.* **51**:12754 – 12758.
http://dx.doi.org/10.1002/anie.201204405.

[28] Symes, M.D., Kitson, P.J., Yan, J., Richmond, C.J., Cooper, G.J.T., Bowman, R.W., Vilbrandt, T. & Cronin, L. (2012) Integrated 3D-printed reactionware for chemical synthesis and analysis. *Nature Chem.* **4**:349 – 354.
http://dx.doi.org/10.1038/nchem.1313.

[29] Kitson, P.J., Rosnes, M.H., Sans, V., Dragone, V. & Cronin, L. (2012) Configurable 3D-Printed millifluidic and microfluidic 'lab on a chip' reactionware devices. *Lab chip* **12**:3267 – 3271.
http://dx.doi.org/10.1039/c2lc40761b.